Available online at www.sciencedirect.com

SCIENCE DIRECT®

Journal of Solid State Chemistry 178 (2005) 1171–1181

JOURNAL OF SOLID STATE CHEMISTRY

www.elsevier.com/locate/jssc

Solvothermal syntheses, crystal structures and properties of five new thioantimonates(III) containing the $[Sb_4S_7]^{2-}$ anion

A. Puls[a], M. Schaefer[a], C. Näther[a], W. Bensch[a,*], A.V. Powell[b], S. Boissière[b], A.M. Chippindale[c]

[a]Institut für Anorganische Chemie, Christian-Albrechts-Universität zu Kiel, Universität Kiel, Olshausenstrabe 40, (Otto-Hahn-Platz 7) D-24098 Kiel, Germany

[b]Department of Chemistry, Heriot-Watt University, Edinburgh EH14 4AS, UK

[c]School of Chemistry, The University of Reading, Whiteknights Reading RG6 6AD, UK

Received 1 December 2004; received in revised form 19 January 2005; accepted 20 January 2005

Abstract

Five new thioantimonates have been synthesized in the presence of organic amines under solvothermal conditions and their structures determined by single-crystal X-ray diffraction. All of the compounds are layered and contain antimony–sulphide anions of stoichiometry $[Sb_4S_7]^{2-}$, but the structure of the anion formed is dependent on the amine used in synthesis. $(H_3N(CH_2)_4NH_3)[Sb_4S_7]$ **(1)** contains $[Sb_4S_7]^{2-}$ double chains directed along [010]. Weak interchain Sb–S interactions between neighbouring chains cause the double chains to pack into layers in the *ab* plane. In the [001] direction, the layers of double chains alternate with doubly protonated diaminobutane molecules to which the chains are hydrogen bonded. Compounds of general formula $(TH)_2[Sb_4S_7]$ ($T = CH_3(CH_2)_2NH_2$ **(2)**, $(CH_3)_2CHNH_2$ **(3)**, $CH_3(CH_2)_3NH_2$ **(4)** and $CH_3(CH_2)_4NH_2$ **(5)**) adopt a more complex structure in which $[Sb_3S_8]^{7-}$ units are linked by SbS_3^{3-} pyramids to form chains, which in turn are bridged by sulphur atoms to create sheets containing large heterorings. Pairs of such sheets form double layers of four atoms thickness that are stacked along [001]. Protonated amine molecules are located between anionic antimony-sulphide layers to which they are hydrogen bonded. Thermal analysis reveals that the decomposition temperature of materials containing $[Sb_4S_7]^{2-}$ anions is dependent both on the structure of the anion, the lowest decomposition temperature being that of the low-dimensional phase **(1)** and on the identity of the amine, the decomposition temperature decreasing with an increasing number of carbon atoms and decreasing density.

Keywords: Solvothermal synthesis; Thioantimonates(III); Thermal stability

1. Introduction

In the field of thioantimonate(III) chemistry, Schäfer and co-workers have synthesized, under solvothermal conditions, a large number of compounds containing alkali or alkaline-earth ions as cationic species for charge balancing anionic sulphide frameworks [1–10]. During the last decade, organic amine cations, transition metals and transition-metal complexes have also been exploited as structure directing agents for the synthesis of new and exciting thioantimonates(III) [11–41]. In this area of synthetic chemistry, several goals are apparent. One is the preparation of open-framework thioantimonates with accessible free voids, cages or holes. Such compounds should be able reversibly to accommodate small molecules, which may induce changes in the physical properties, leading to potential applications as sensors, for example [42]. Another goal is the synthesis of inorganic–organic hybrid materials, in which interaction at the microscopic level between inorganic and organic fragments, may confer on the hybrid, properties which differ markedly from those of either component. In layered thioantimonates(III), the arrangement of the organic molecules between the layers

*Corresponding author. Fax: +49 431 880 1520.
E-mail address: wbensch@ac.uni-kiel.de (W. Bensch).

0022-4596/$ - see front matter © 2005 Elsevier Inc. All rights reserved.
doi:10.1016/j.jssc.2005.01.019

may lead to pillaring and, under certain circumstances, an open space between neighbouring pillars is formed [22]. Furthermore, as the mechanism of these heterogeneous multi-component reactions is not well understood, exploratory synthesis is necessary in order to acquire a knowledge of which parameters determine, for instance, the architecture of the product and, in particular, the dimensionality of the thioantimonate(III) network.

In most thioantimonates(III) containing organic amine cations, in addition to an electrostatic interaction between the negatively charged $[Sb_xS_y]^{z-}$ networks and the charge compensating counterions, S···H hydrogen bonding also plays a key role in holding the structure together. Although individually weak, there are generally a large number of such S···H bonds, which cannot therefore be neglected. Examination of the crystal structures of organically templated thioantimonates(III) shows that the NH_3 groups of the amino cations adopt a special arrangement with respect to the S atoms of the thioantimonate network to allow hydrogen bonding to take place [16,28,35,36].

Anions of stoichiometry $[Sb_4S_7]^{2-}$ are particularly prevalent in thioantimonates and examples include $K_2Sb_4S_7$ [1], $(NH_4)_2Sb_4S_7$ [2], $Rb_2Sb_4S_7 \cdot H_2O$ [4], $Cs_2Sb_4S_7$ [5], $K_2Sb_4S_7 \cdot H_2O$ [6], $SrSb_4S_7 \cdot 6H_2O$ [7], $Rb_2Sb_4S_7$ [26], $(C_4N_2H_8)Sb_4S_7$ [33], $[M(en)_3]Sb_4S_7$ (M = Mn, Fe, Co, Ni) [29,41,43], $(C_2H_5NH_3)_2Sb_4S_7$ [37], $[Ni(dien)_2]Sb_4S_7 \cdot H_2O$ [39], $[Mn(dien)_2]Sb_4S_7$ [40] and $(C_6H_{20}N_4)[Sb_4S_7]$ [43]. Of these, only $K_2Sb_4S_7$ [1] shows a three-dimensional $[Sb_4S_7]^{2-}$ anionic framework and, with increasing size of the cation, the dimensionality is reduced to two-dimensional layers and finally to one-dimensional chains [41,44]. However, a serious problem with the assignment of the dimensionality is the fact that Sb–S distances show no clear cut-off in the large range between 2.2 and 4.0 Å. Therefore, there is a degree of arbitrariness in the description of the structures of thioantimonates(III), and hence the assignment of the dimensionality should be treated with caution.

A few years ago, one of us reported the synthesis and crystal structure of $(eaH)_2[Sb_4S_7]$ (ea = ethylamine) [37], which shows a new architecture compared to the known thioantimonates(III). In our ongoing work, we continue to investigate the influence of the size of organic amine cations on the dimensionality of thioantimonate frameworks and on the interconnection of the SbS_x primary building units. Here we report the syntheses, crystal structures and thermal stability of five new thioantimonates(III) containing an $[Sb_4S_7]^{2-}$ anionic framework.

2. Experimental section

2.1. Syntheses

The title compounds were prepared in 30 ml Teflon-lined stainless-steel autoclaves. The compound $(dabH_2)Sb_4S_7$ **(1)** was synthesized from Sb_2S_3 and 1,4-diaminobutane (dab) in water in a molar ratio of Sb_2S_3:dab:H_2O of 1:4:30. For the syntheses of $(paH)_2Sb_4S_7$ **(2)**, $(ipaH)_2Sb_4S_7$ **(3)**, $(baH)_2Sb_4S_7$ **(4)** and $(peaH)_2Sb_4S_7$ **(5)**, a molar ratio of 1:3 for Sb:S (mmol scale) was used and 3 ml of *n*-propylamine (pa), isopropylamine (ipa), *n*-butylamine (ba), and *n*-pentylamine (pea), respectively was added as solvent. The slurries were heated at 130 °C (**(2)** and **(4)**) and at 170 °C (**(3)** and **(5)**) for 14 days and 160 °C **(1)** for 21 days. Compounds **(2)** and **(3)** were obtained as red needles (yield 40% and 70%, respectively, based on Sb) whilst **(1)** (yield 40%) **(4)** (yield 40%) and **(5)** (yield 30%) crystallize as orange needles. When lower temperatures were used during the syntheses, the products consisted of either poor quality crystals or microcrystalline powders. The yield of compounds **(2)–(5)** can be dramatically increased when the slurries are stirred during the reaction.

2.1.1. CHN analyses

(1) Calc. %C = 5.99; %N = 3.49; %H = 1.76; found: %C = 5.36% N = 3.27% H = 1.85; **(2)** Calc. %C = 8.66; %N = 3.37; %H = 2.405; found: %C = 8.775; %N = 3.27%H = 2.061; **(3)** Calc. %C = 8.66; %N = 3.37; %H = 2.405; found: %C = 7.92; %N = 3.102; %H = 2.20; **(4)** Calc. %C = 11.17; %N = 3.26; %H = 2.792; found: %C = 11.256; %N = 3.151; %H = 2.697; **(5)** Calc. %C = 13.52%; %N = 3.15%; H = 3.154; found: %C = 12.984; %N = 2.985; %H = 2.725

Reaction of elemental Sb, Zn, and S in the molar ratio 1:1:2.5 in 3 ml 80% aqueous solution of tris(2-aminoethylene)amine at 140 °C for 7 days produced $(trenH_2)Sb_4S_7$, identical with that previously reported [43]. It is interesting to note that both in the present work and in that previously reported, the presence of a transition metal is essential for the successful synthesis of this phase.

2.2. Crystallography

Single-crystal X-ray intensity data were collected at room temperature on a STOE IPDS I Imaging Plate Diffraction System (Compounds **(2)**, **(3)**, **(5)**), a STOE AED II (Compound **(4)**) and a Nonius Kappa CCD diffractometer (Compound **(1)**), all with graphite monochromated MoK_α radiation ($\lambda = 0.71073$ Å). The raw intensities were treated in the usual way particular to each instrument by applying Lorentz, polarization and absorption corrections. Structure solution was performed with either SHELXS-97 [45] (Compounds **(2)–(5)**) or SIR92 [46] (Compound **(1)**). Refinement was performed against F^2 using SHELXL-97 [47] for Compounds **(2)–(5)** and against F using the CRYSTALS suite of programs [48] (Compound **(1)**). In Compounds **(4)** and **(5)**, two and three C atoms, respectively, within the amine chains are disordered over two positions with 50:50 site occupation. The crystal of compound **(2)** was non-merohedrically twinned. The reflections of both individuals were indexed and integrated separately. All non-hydrogen atoms were refined with anisotropic displacement parameters. Hydrogen atoms were either placed geometrically and their positions refined using a riding model or they were placed geometrically after each cycle of refinement. Crystallographic data for Compounds **(1)**–**(5)** are summarized in Table 1 and selected bond lengths and angles are given in Table 2. Atomic coordinates and isotropic displacement parameters are presented in Table 3.

Crystallographic data (excluding structure factors) have been deposited with the Cambridge Crystallographic Data Centre as supplementary publication no. CCDC 256025 **(1)** CCDC 253611 **(2)**, CCDC 253612 **(3)**, CCDC 253613 **(4)** and CCDC 253614 **(5)**. Copies of the data can be obtained, free of charge, on application to CCDC, 12 Union Road, Cambridge CB2 1 EZ, UK. (fax: +44-(0)1223-336033 or email: deposit@ccdc.cam.ac.uk).

2.3. Thermal investigations

The thermal measurements were performed on a Netzsch STA 429 DTA-TG instrument. The samples were heated to 400 °C in Al_2O_3 crucibles at a rate of 3 °C min^{-1} and purged in an argon stream of approximately 50 mL min^{-1}. DTA-TG-MS measurements were conducted simultaneously using a STA-409CD device (Netzsch) with Skimmer coupling, which is equipped with a Balzers QMA 400 Quadrupole Mass Spectrometer (max. 512 amu). The MS measurements were performed in the analogue and trend scan modes. All measurements were corrected for buoyancy and current effects and were carried out with heating rates of 4 °C min^{-1} in Al_2O_3 crucibles under a dynamic nitrogen atmosphere (flow-rate: 75 mL min^{-1}, purity: 5.0).

3. Results and discussion

All compounds $(dabH_2)Sb_4S_7$ **(1)**, $(paH)_2Sb_4S_7$ **(2)**, $(ipaH)_2Sb_4S_7$ **(3)**, $(baH)_2Sb_4S_7$ **(4)**, and $(peaH)_2Sb_4S_7$ **(5)** crystallize in the triclinic space group *P*-1 with two formula units in the unit cell. The crystallographically independent atoms are all located on general positions. All of the structures consist of alternating anionic $[Sb_4S_7]^{2-}$ layers separated by organic cations, which also show layer-like arrangements. Despite the identical stoichiometry of the thioantimonate(III) anions, they are not isostructural and two different binding modes of the SbS_3 pyramids and SbS_4 units are observed in **(1)**–**(5)**, respectively.

Table 1
Crystallographic details for compounds $(dabH_2)Sb_4S_7$ **(1)**, $(paH)_2Sb_4S_7$ **(2)**, $(ipaH)_2Sb_4S_7$ **(3)**, $(baH)_2Sb_4S_7$ **(4)**, and $(peaH)_2Sb_4S_7$ **(5)**

	$(dabH_2)Sb_4S_7$ **(1)**	$(paH)_2Sb_4S_7$ **(2)**	$(ipaH)_2Sb_4S_7$ **(3)**	$(baH)_2Sb_4S_7$ **(4)**	$(peaH)_2Sb_4S_7$ **(5)**
Crystal system	Triclinic	Triclinic	Triclinic	Triclinic	Triclinic
a/Å	6.0166(3)	7.0123(5)	7.0421(5)	7.038(1)	7.0153(5)
b/Å	8.9747(3)	11.9296(9)	11.9297(9)	11.950(2)	11.9169(9)
c/Å	16.5486(7)	14.2666(10)	14.1285(10)	15.501(3)	16.7426(12)
α/°	89.742(2)	114.064(8)	114.320(8)	67.9(1)	109.179(8)
β/°	86.329(2)	98.434(8)	99.429(9)	77.3(1)	99.745(9)
γ/°	84.602(1)	92.605(8)	92.339(9)	87.3(1)	92.817(9)
V/Å^3	887.79(7)	1070.60(13)	1059.23(13)	1177.5(3)	1294.65(16)
Space group	$P-1$	$P-1$	$P-1$	$P-1$	$P-1$
Z	2	2	2	2	2
Calc. density/g cm^{-3}	2.999	2.580	2.608	2.425	2.277
Crystal colour	Orange	Orange	Red	Orange	Red
μ/mm^{-1}	6.825	5.66	5.73	5.155	4.692
Scan range	$10° \leqslant 2\theta \leqslant 55°$	$3° \leqslant 2\theta \leqslant 52°$	$6° \leqslant 2\theta \leqslant 56°$	$6° \leqslant 2\theta \leqslant 60°$	$5° \leqslant 2\theta \leqslant 56°$
Index range	$-7 \leqslant h \leqslant 7$	$-7 \leqslant h \leqslant 7$	$-9 \leqslant h \leqslant 9$	$0 \leqslant h \leqslant 9$	$-8 \leqslant h \leqslant 9$
	$-11 \leqslant k \leqslant 11$	$-14 \leqslant k \leqslant 14$	$-15 \leqslant k \leqslant 15$	$-16 \leqslant k \leqslant 16$	$-15 \leqslant k \leqslant 5$
	$-21 \leqslant l \leqslant 20$	$-17 \leqslant l \leqslant 17$	$-18 \leqslant l \leqslant 18$	$-21 \leqslant l \leqslant 21$	$-22 \leqslant l \leqslant 21$
Reflections collected	5957	5166	9939	7526	12277
Independent reflections	3881	2445	4795	6846	6127
R_{int}	0.046	0.0365	0.0759	0.0248	0.0358
Temperature/K	293	293	293	293	293
Min./max. transmission	0.19/0.93	0.38/0.54	–	0.38/0.57	0.42/0.56
refl. with $F_o > 4\sigma(F_o)$	2773	2200	3622	5626	5144
Number of parameters	154	173	163	208	211
R_1 for $F_o > 4\sigma(F_o)$	0.0459	0.0259	0.0423	0.0265	0.0366
WR_2 for all reflections	0.0517	0.0692	0.1077	0.0691	0.1049
GOOF	1.0846	1.048	1.006	0.994	1.085
$\Delta\rho$ [e/Å^3]	−1.79/1.6	−0.63/0.48	−1.95/0.97	−0.97/1.05	−1.184/1.191

Table 2
Bond lengths (Å) for $(dabH_2)Sb_4S_7$ **(1)**, $(paH)_2Sb_4S_7$ **(2)**, $(i paH)_2Sb_4S_7$ **(3)**, $(baH)_2Sb_4S_7$ **(4)**, and $(peaH)_2Sb_4S_7$ **(5)**

$(dabH_2)Sb_4S_7$ **(1)**			
Sb(1)–S(5)	2.413(1)	Sb(2)–S(1)	2.505(2)
Sb(1)–S(5)^{I}	2.740(2)	Sb(2)–S(2)	2.509(2)
Sb(1)–S(6)	2.576(2)	Sb(2)–S(7)	2.419(2)
Sb(1)–S(7)	2.735(2)	Sb(3)–S(5)	2.486(2)
Sb(3)–S(2)	2.463(2)	Sb(4)–S(1)^{iii}	2.459(2)
Sb(3)–S(3)	2.389(2)	Sb(4)–S(4)	2.501(2)
Sb(3)–S(4)^{ii}	2.471(2)	Sb(4)–S(6)	2.489(2)
Sb(1)–S(1)^{iv}	3.080(2)	Sb(4)–S(7)^{vi}	3.079(2)
Sb(2)–S(5)	3.184(2)	Sb(4)–S(5)^{v}	3.156(2)
Sb(3)–S(7)	3.329(2)		
Symmetry codes: (i) $1-x$, $2-y$, $1-z$; (ii) x, $y-1$, z; (iii) x, $1+y$, z; (iv) $1-x$, $1-y$, $1-z$; (v) $1-x$, $2-y$, $1-z$; (vi) x, $1+y$, z			
$(paH)_2Sb_4S_7$ **(2)**			
Sb(1)–S(1)	2.391(1)	2.577(2)	
Sb(1)–S(3)^{i}	2.454(2)	3.028(2)	
Sb(2)–S(2)	2.414(2)	2.465(2)	
Sb(2)–S(4)	2.442(1)	2.525(2)	
Sb(3)–S(5)	2.487(1)	2.414(2)	
Sb(3)–S(6)^{ii}	3.061(2)	2.655(2)	
Sb(4)–S(5)^{ii}	2.459(2)	2.766(2)	
Sb(4)–S(7)	2.417(2)		
Sb(1)–S(7)	3.847(2)	3.383(2)	
Sb(2)–S(7)^{v}	3.749(2)	3.296(2)	
Sb(4)–S(6)^{iv}	3.637(2)	3.808(2)	
Symmetry codes: (i) $1+x$, y, z; (ii) $1-x$, $1-y$, $1-z$; (iii) $2-x$, $2-y$, $1-z$; (iv) $2-x$, $1-y$, $1-z$; (v) $1-x$, $2-y$, $1-z$			
$(i paH)_2Sb_4S_7$ **(3)**			
Sb(1)–S(1)	2.3993(19)	2.599(2)	
Sb(1)–S(3)^{i}	2.461(2)	3.013(2)	
Sb(2)–S(2)	2.419(2)	2.473(2)	
Sb(2)–S(4)	2.4476(19)	2.543(2)	
Sb(3)–S(5)	2.4937(19)	2.4218(18)	
Sb(3)–S(6)^{ii}	3.050(2)	2.679(2)	
Sb(4)–S(5)^{ii}	2.461(2)	2.771(2)	
Sb(4)–S(7)	2.419(2)		
Sb(1)–S(7)	3.956(2)	3.401(2)	
Sb(2)–S(7)^{v}	3.740(2)	3.291(2)	
Sb(4)–S(6)^{iv}	3.621(2)	3.814(2)	
Symmetry codes: (i) $1+x$, y, z; (ii) $1-x$, $1-y$, $1-z$; (iii) $2-x$, $2-y$, $1-z$; (iv) $2-x$, $1-y$, $1-z$; (v) $1-x$, $2-y$, $1-z$			
$(baH)_2Sb_4S_7$ **(4)**			
Sb(1)–S(1)	2.397(1)	2.584(1)	
Sb(1)–S(3)^{iii}	2.453(1)	3.006(1)	
Sb(2)–S(2)	2.414(1)	2.468(1)	
Sb(2)–S(4)	2.4387(9)	2.529(1)	
Sb(3)–S(5)	2.4858(9)	2.4164(9)	
Sb(3)–S(6)^{i}	3.061(1)	2.637(1)	
Sb(4)–S(5)^{i}	2.464(1)	2.784(1)	
Sb(4)–S(7)	2.4248(9)		
Sb(1)–S(7)	3.867(1)	3.394(1)	
Sb(2)–S(7)^{iv}	3.786(1)	3.309(1)	
Sb(4)–S(6)^{v}	3.613(1)	3.851(1)	
Symmetry codes: (i) $1-x$, $2-y$, $-z$; (ii) $2-x$, $1-y$, $-z$; (iii) $1+x$, y, z; (iv) $1-x$, $1-y$, $-z$; (v) $2-x$, $2-y$, $-z$			
$(peaH)_2Sb_4S_7$ **(5)**			
Sb(1)–S(1)	2.3919(14)	2.5681(15)	
Sb(1)–S(3)^{I}	2.4477(15)	3.0113(5)	
Sb(2)–S(2)	2.4097(14)	2.4604(15)	
Sb(2)–S(4)	2.4371(14)	2.5234(15)	
Sb(3)–S(5)	2.4803(14)	2.4122(16)	
Sb(3)–S(6)^{ii}	3.0569(15)	2.6315(15)	
Sb(4)–S(5)^{ii}	2.4582(14)	2.7827(15)	
Sb(4)–S(7)	2.4208(14)		
Sb(1)–S(7)	3.8394(15)	3.3851(15)	

Table 2 (*continued*)

Sb(2)–S(7)^{v}	3.7683(14)	3.2932(15)	
Sb(4)–S(6)^{iv}	3.6164(14)	3.8286(15)	
Symmetry codes: (i) $1+x$, y, z; (ii) $1-x$, $1-y$, $1-z$; (iii) $2-x$, $2-y$, $1-z$; (iv) $2-x$, $1-y$, $1-z$; (v) $1-x$, $2-y$, $1-z$			
$(dabH_2)Sb_4S_7$ **(1)**			
S(5)–Sb(1)–S(5)^{I}	86.11(6)	S(2)–Sb(3)–S(3)	92.18(8)
S(5)–Sb(1)–S(6)	93.36(7)	S(2)–Sb(3)–S(4)^{ii}	98.84(7)
S(5)^{i}–Sb(1)–S(6)	93.64(6)	S(3)–Sb(3)–S(4)^{ii}	98.80(9)
S(5)^{i}–Sb(1)–S(7)	168.00(6)	S(1)^{iii}–Sb(4)–S(4)	94.51(8)
S(6)–Sb(1)–S(7)	96.89(7)	S(1)^{iii}–Sb(4)–S(6)	90.32(7)
S(1)–Sb(2)–S(2)	94.31(7)	S(4)–Sb(4)–S(6)	91.46(7)
S(1)–Sb(2)–S(7)	91.95(7)	S(1)–Sb(1)–S(2)	89.20(7)
S(2)–Sb(2)–S(7)	95.28(7)		
Symmetry codes: (i) $1-x$, $2-y$, $1-z$; (ii) x, $y-1$, z; (iii) x, $1+y$, z;			
$(paH)_2Sb_4S_7$ **(2)**			
S(1)–Sb(1)–S(3)^{I}	97.43(6)	S(1)–Sb(1)–S(2)	89.63(5)
S(3)^{i}–Sb(1)–S(2)	86.98(5)	S(2)–Sb(2)–S(4)	94.86(6)
S(2)–Sb(2)–S(3)	93.36(6)	S(4)–Sb(2)–S(3)	89.94(5)
S(6)–Sb(3)–S(5)	91.15(5)	S(6)–Sb(3)–S(4)	97.21(5)
S(5)–Sb(3)–S(4)	85.58(5)	S(7)–Sb(4)–S(5)^{ii}	109.90(5)
S(7)–Sb(4)–S(1)^{iii}	87.85(5)	S(5)^{ii}–Sb(4)–S(1)^{iii}	81.34(5)
S(7)–Sb(4)–S(6)	87.32(5)	S(5)^{ii}–Sb(4)–S(6)	88.59(5)
Symmetry codes: (i) $1+x$, y, z; (ii) $1-x$, $1-y$, $1-z$; (iii) $2-x$, $2-y$, $1-z$			
$(i\text{pa}H)_2Sb_4S_7$ **(3)**			
S(1)–Sb(1)–S(3)^{I}	97.29(8)	S(1)–Sb(1)–S(2)	89.94(7)
S(3)$^{i-}$Sb(1)–S(2)	86.64(7)	S(2)–Sb(2)–S(4)	94.04(7)
S(2)–Sb(2)–S(3)	93.72(8)	S(4)–Sb(2)–S(3)	90.42(7)
S(6)–Sb(3)–S(5)	91.00(7)	S(6)–Sb(3)–S(4)	96.72(7)
S(5)–Sb(3)–S(4)	85.46(7)	S(7)–Sb(4)–S(5)^{ii}	109.30(8)
S(7)–Sb(4)–S(1)^{iii}	88.09(7)	S(5)$^{ii-}$Sb(4)–S(1)^{iii}	81.70(7)
S(7)–Sb(4)–S(6)	87.54(6)	S(5)$^{ii-}$Sb(4)–S(6)	87.86(6)
Symmetry codes: (i) $1+x$, y, z; (ii) $1-x$, $1-y$, $1-z$; (iii) $2-x$, $2-y$, $1-z$			
$(baH)_2Sb_4S_7$ **(4)**			
S(1)–Sb(1)–S(3)^{iii}	97.11(3)	S(1)–Sb(1)–S(2)	89.20(3)
S(3)$^{iii-}$Sb(1)–S(2)	87.45(3)	S(2)–Sb(2)–S(4)	94.69(3)
S(2)–Sb(2)–S(3)	93.50(3)	S(4)–Sb(2)–S(3)	90.05(3)
S(6)–Sb(3)–S(4)	97.90(3)	S(6)–Sb(3)–S(5)	91.40(3)
S(5)–Sb(3)–S(4)	85.57(3)	S(7)–Sb(4)–S(5)^{i}	110.38(3)
S(5)$^{i-}$Sb(4)–S(6)	88.93(3)	S(7)–Sb(4)–S(1)^{ii}	87.64(3)
S(5)$^{i-}$Sb(4)–S(1)^{ii}	81.85(3)	S(7)–Sb(4)–S(6)	86.47(3)
Symmetry codes: (i) $1-x$, $2-y$, $-z$; (ii) $2-x$, $1-y$, $-z$; (iii) $1+x$, y, z			
$(peaH)_2Sb_4S_7$**(5)**			
S(1)–Sb(1)–S(3)^{I}	97.17(6)	S(1)–Sb(1)–S(2)	89.41(5)
S(3)$^{i-}$Sb(1)–S(2)	87.33(5)	S(2)–Sb(2)–S(4)	94.54(5)
S(2)–Sb(2)–S(3)	93.68(5)	S(4)–Sb(2)–S(3)	89.97(5)
S(6)–Sb(3)–S(5)	91.29(5)	S(6)–Sb(3)–S(4)	97.79(6)
S(5)–Sb(3)–S(4)	85.49(5)	S(7)–Sb(4)–S(5)^{ii}	110.47(5)
S(7)–Sb(4)–S(1)^{iii}	87.67(5)	S(5)$^{ii-}$Sb(4)–S(1)^{iii}	81.46(5)
S(7)–Sb(4)–S(6)	86.73(5)	S(5)$^{ii-}$Sb(4)–S(6)	88.86(4)
Symmetry codes: (i) $1+x$, y, z; (ii) $1-x$, $1-y$, $1-z$; (iii) $2-x$, $2-y$, $1-z$			

Estimated standard deviations are given in parentheses.

In the following discussion, the descriptions of the structures are based on a cut-off of ca. 3.1 Å for the Sb–S distances. In **(1)**, Sb(2), Sb(3) and Sb(4) are each coordinated to three sulphur atoms at distances in the range 2.419(2)–2.509(2) Å to form trigonal pyramidal units (Fig. 1). These three SbS_3^{3-} groups share common corners to form an $Sb_3S_6^{3-}$ secondary building unit (SBU) termed a semicube. The remaining antimony atom, Sb(1), has two short ($\leqslant$2.6 Å) and two longer ($\geqslant$2.73 Å) bonds to sulphur forming an SbS_4^{5-} moiety, which connects the $Sb_3S_6^{3-}$ SBUs to form an $[Sb_4S_7]^{2-}$ chain. Two SbS_4^{5-} units in adjacent chains share a common edge yielding an Sb_2S_2 ring that serves to link pairs of chains to form $Sb_4S_7^{2-}$ double chains that are

Table 3
Atomic coordinates (10^4) and equivalent isotropic displacement parameters U_{eq} ($Å^2 \times 10^3$) in for $(dabH_2)Sb_4S_7$ **(1)**, $(paH)_2Sb_4S_7$ **(2)**, $(i paH)_2Sb_4S_7$ **(3)**, $(baH)_2Sb_4S_7$ **(4)**, and $(peaH)_2Sb_4S_7$ **(5)**

	x	*y*	*z*	U_{eq}
$(dabH_2)Sb_4S_7$ **(1)**				
Sb(1)	2704(1)	8790(1)	4789(1)	22
Sb(2)	6538(1)	5274(1)	3774(1)	23
Sb(3)	1695(1)	6223(1)	2354(1)	24
Sb(4)	1823(1)	12695(1)	3814(1)	22
S(1)	5914(1)	2580(2)	3588(1)	23
S(2)	5809(3)	5982(2)	2340(1)	26
S(3)	1755(4)	6569(3)	921(1)	34
S(4)	1080(4)	13540(2)	2406(1)	27
S(5)	6703(3)	8542(2)	4495(1)	22
S(6)	1909(3)	10003(2)	3410(1)	24
S(7)	2719(3)	5881(2)	4302(1)	24
N(1)	7174(12)	9459(8)	2550(4)	27
N(2)	2984(13)	13473(9)	–154(5)	35
C(1)	7431(12)	10400(10)	1813(5)	29
C(2)	5174(13)	10623(11)	1418(5)	34
C(3)	5244(15)	11900(11)	796(6)	38
C(4)	3043(14)	12120(10)	370(6)	34
$(paH)_2Sb_4S_7$ **(2)**				
Sb(1)	8846(1)	10147(1)	3767(1)	25(1)
Sb(2)	3616(1)	8577(1)	3633(1)	24(1)
Sb(3)	3781(1)	5924(1)	4331(1)	24(1)
Sb(4)	9416(1)	6606(1)	5332(1)	27(1)
S(1)	8460(2)	11583(1)	2994(1)	34(1)
S(2)	5756(2)	8805(1)	2526(1)	30(1)
S(3)	692(2)	8751(1)	2532(1)	32(1)
S(4)	3020(2)	6327(1)	2718(1)	31(1)
S(5)	1527(2)	3990(1)	3326(1)	29(1)
S(6)	6552(2)	4822(1)	3880(1)	28(1)
S(7)	7433(2)	8132(1)	5141(1)	34(1)
N(1)	3685(11)	1476(7)	2549(6)	56(2)
C(1)	2900(20)	881(14)	1472(11)	95(4)
C(2)	3480(30)	1490(20)	844(15)	167(9)
C(3)	2480(30)	1330(40)	(20)	250(19)
N(2)	7969(10)	6165(5)	2404(5)	46(2)
C(4)	7400(20)	5417(11)	1298(10)	94(4)
C(5)	8070(30)	4232(16)	934(17)	188(13)
C(6)	7580(40)	3321(19)	40(20)	198(12)
$(i paH)_2Sb_4S_7$ **(3)**				
Sb(1)	8849(1)	10143(1)	3719(1)	24(1)
Sb(2)	3641(1)	8574(1)	3583(1)	22(1)
Sb(3)	3769(1)	5938(1)	4327(1)	19(1)
Sb(4)	9425(1)	6609(1)	5353(1)	23(1)
S(1)	8367(3)	11571(2)	2928(2)	29(1)
S(2)	5751(3)	8732(2)	2443(2)	29(1)
S(3)	692(3)	8764(2)	2465(2)	32(1)
S(4)	3000(3)	6313(2)	2666(2)	25(1)
S(5)	1488(3)	3996(2)	3299(2)	25(1)
S(6)	6521(3)	4815(2)	3879(2)	23(1)
S(7)	7428(3)	8143(2)	5181(2)	33(1)
N(1)	3463(13)	1378(8)	2349(7)	43(2)
C(1)	2630(20)	1149(12)	1252(11)	59(3)
C(2)	3530(30)	2062(14)	942(14)	90(6)
C(3)	2640(20)	(13)	542(12)	69(4)
N(2)	7983(11)	6035(7)	2345(6)	33(2)
C(4)	7249(15)	5161(10)	1223(9)	47(2)
C(5)	7760(19)	5751(12)	518(9)	54(3)
C(6)	8100(02)	3952(10)	991(12)	67(4)

Table 3 (*continued*)

	x	*y*	*z*	U_{eq}
$(baH)_2Sb_4S_7$ **(4)**				
Sb(1)	3730(1)	8448(1)	625(1)	25(1)
Sb(2)	3557(1)	5150(1)	1247(1)	26(1)
Sb(3)	9458(1)	8736(1)	(1)	28(1)
Sb(4)	8791(1)	3703(1)	1122(1)	27(1)
S(1)	6474(1)	9147(1)	1015(1)	28(1)
S(2)	1407(1)	9423(1)	1560(1)	30(1)
S(3)	2886(1)	6530(1)	2094(1)	31(1)
S(4)	560(1)	3945(1)	2244(1)	34(1)
S(5)	5609(1)	3889(1)	2258(1)	33(1)
S(6)	7469(1)	7015(1)	(1)	33(1)
S(7)	8343(1)	1547(1)	1843(1)	33(1)
N(1)	3575(6)	1242(3)	2215(3)	50(1)
C(1)	2672(8)	823(5)	3228(4)	61(1)
C(2)	3469(10)	(6)	3776(5)	84(2)
C(3)	2491(13)	(9)	4847(6)	128(4)
C(4)	3161(16)	(10)	5425(7)	169(6)
N(2)	7824(6)	6429(3)	2321(3)	47(1)
C(11)	7176(19)	5998(13)	3337(8)	60(3)
C(12)	7970(20)	6790(20)	3737(11)	105(6)
C(11’)	7290(19)	6688(12)	3238(9)	58(3)
C(12’)	7870(19)	5640(15)	4033(9)	75(3)
C(13)	7451(15)	6050(15)	4922(7)	166(6)
C(14)	8530(20)	6731(17)	5145(12)	213(8)
$(peaH)_2Sb_4S_7$ **(5)**				
Sb(1)	8830(1)	10273(1)	3984(1)	25(1)
Sb(2)	3596(1)	8721(1)	3873(1)	25(1)
Sb(3)	3762(1)	5989(1)	4437(1)	24(1)
Sb(4)	9440(1)	6568(1)	5291(1)	27(1)
S(1)	8438(2)	11787(1)	3339(1)	32(1)
S(2)	5706(2)	9070(1)	2962(1)	31(1)
S(3)	642(2)	9014(1)	2971(1)	33(1)
S(4)	2974(2)	6571(1)	3109(1)	31(1)
S(5)	1468(2)	4169(1)	3600(1)	28(1)
S(6)	6514(2)	4928(1)	4078(1)	27(1)
S(7)	7454(2)	8106(1)	5112(1)	32(1)
N(1)	7901(9)	6459(6)	2900(4)	47(1)
C(1)	7280(20)	5909(13)	1974(8)	62(3)
C(1’)	7390(50)	5310(20)	2100(20)	52(9)
C(2)	8060(20)	4812(16)	1603(10)	87(5)
C(2’)	7930(80)	5620(50)	1360(30)	90(14)
C(3)	7390(30)	4328(16)	616(11)	125(5)
C(4)	8430(40)	3440(20)	198(17)	190(10)
C(5)	7650(40)	2840(20)	(11)	183(10)
N(2)	3692(10)	1780(6)	3017(4)	49(2)
C(6)	2873(17)	1277(10)	2116(6)	74(3)
C(7)	3540(20)	1873(16)	1587(8)	108(5)
C(8)	2520(30)	1100(20)	621(10)	108(6)
C(8’)	2890(1 0 0)	2150(60)	810(40)	105(17)
C(9)	3240(40)	1450(20)	33(17)	183(9)
C(10)	2350(30)	820(20)	(10)	182(10)

Estimated standard deviations are given in parentheses. The equivalent isotropic displacement parameter is defined as one third of the trace of the orthogonalised U_{ij} tensor.

directed along [010]. The linkage of $Sb_3S_6^{3-}$ semicubes and Sb_2S_2 rings generates larger Sb_4S_4 heterorings (Fig. 1). Whereas six S atoms connect two Sb atoms, which may be formulated as $S^{[2]}$ atoms, the S(3) atom is terminal ($S^{[1]}$ mode).

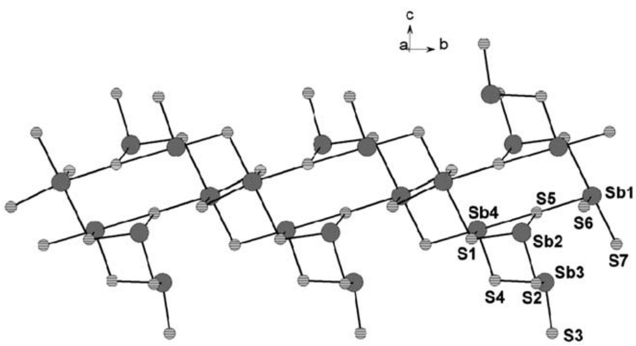

Fig. 1. Interconnection of the primary SbS_3^{3-} and SbS_4^{5-} units together with atom labelling scheme in **(1)**.

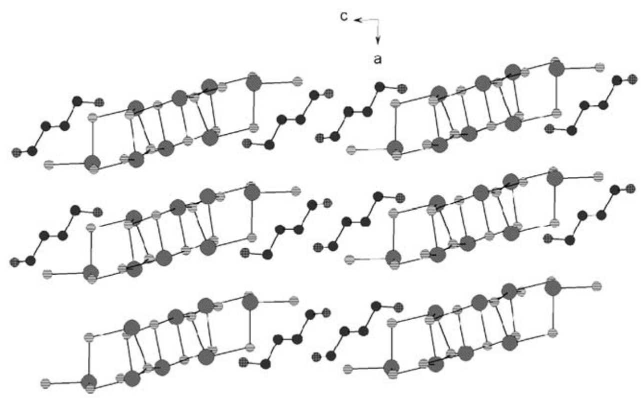

Fig. 2. The arrangement of the anionic $Sb_4S_7^{2-}$ double chains and the doubly protonated diaminobutane molecules in **(1)**.

Secondary Sb–S interactions at distances within the sum of the van der Waals' radii link the two-atom thick $Sb_4S_7^{2-}$ double chains into layers within the (001) plane (Fig. 2) with neighbouring chains lying in the [100] and [001] directions. The shortest separation along [100] is ca. 3.57 Å, whilst along [001], neighbouring anions are separated by pairs of diprotonated diaminobutane molecules, resulting in a significantly longer anion-anion distance of ca. 6.49 Å. Each of the two crystallographically distinct nitrogen atoms has sulphur neighbours at distances in the range 3.29–3.34 Å, suggesting the presence of hydrogen bonding between anions and template, as observed in other thioantimonates(III) [13,16,17,35].

Compounds **(2)–(5)** all exhibit the same antimony–sulphide network topology, which is distinct from that found in $(dabH_2)Sb_4S_7$ **(1)** but similar to that reported for $(C_2H_5NH_3)_2[Sb_4S_7]$ [37]. In these compounds, the primary building units (PBUs) are one SbS_3^{3-} trigonal pyramid (Sb(2)) and three SbS_4^{5-} units. The Sb–S bond lengths in the SbS_3^{3-} pyramids and in the SbS_4^{5-} moieties, as well as the S–Sb–S angles, are in the typical range observed previously in extended thioantimonates(III) (Table 2) [1–40]. Individual Sb–S bonds exhibit small differences within the four compounds, but there is no obvious trend. The Sb atoms complete their coordination spheres via secondary bonds to S atoms (Table 2) forming a ψ-trigonal bipyramid (Sb(1)) and distorted ψ-octahedra for the other unique Sb atoms. The $Sb(3)S_4^{5-}$ group is edge-linked to two other SbS_4^{5-} moieties forming an $Sb_3S_8^{7-}$ unit as an SBU. These SBUs are joined by SbS_3^{3-} pyramids sharing vertices to form a chain of alternating $Sb_3S_8^{7-}$ and SbS_3^{3-} units (Fig. 3). Neighbouring chains are connected via S(3) of the SbS_3^{3-} pyramid to form, within the *ab* crystallographic plane, sheets that contain relatively large $Sb_{10}S_{10}$ heterorings (Fig. 3). These sheets are then further connected through S(6), the binding mode of which is therefore of $S^{[3]}$-type, so that double sheets, 4 atoms thick, of condensed heterorings are formed (Fig. 4). The condensation leads to the formation of small Sb_2S_2 rings (Fig. 4). Within these double sheets, six edge-linked SbS_4^{5-} units form a complex $Sb_6S_{14}^{6-}$ building block (Fig. 4). It should be noted that in compounds **(2)–(5)**, six S atoms act in an

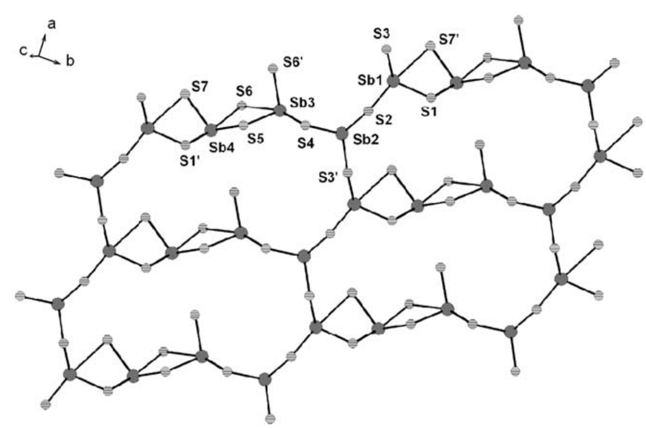

Fig. 3. Interconnection of the primary building units in compounds **(2)–(5)** with labelling. An individual sheet is formed containing the $Sb_{10}S_{10}$ heteroring. The primed atoms are generated by symmetry.

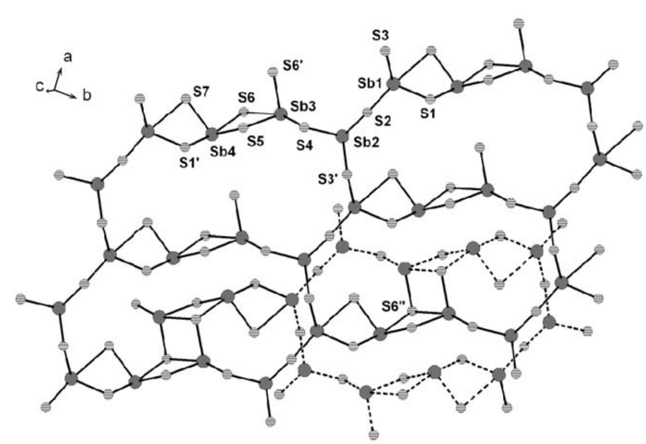

Fig. 4. In compounds **(2)–(5)**, two sheets are joined by the S(6) atom. One ring in the lower sheet is shown with dotted bonds between Sb and S. Note: to reduce overlap of the atoms, the view shown is not exactly parallel to [010].

$S^{[2]}$ mode and one (S(6)) is $S^{[3]}$, in contrast to **(1)**, where in addition to the six $S^{[2]}$-type atoms, there is one S atom exhibiting an $S^{[1]}$ mode.

The individual sheets are stacked along [001]. The shortest interlayer spacings are ca. 7.81 Å for $(paH)_2[Sb_4S_7]$, 7.52 Å for $(ipaH)_2[Sb_4S_7]$, 8.34 Å for $(baH)_2[Sb_4S_7]$ and 9.90 Å for $(peaH)_2[Sb_4S_7]$ (Fig. 5). The interlayer distance for the previously prepared compound $(eaH)_2[Sb_4S_7]$ is ca. 6.56 Å [37]. These large interlayer separations result from the arrangement of the organic cations, which form double layers with the protonated amine groups pointing towards the thioantimonate(III) layers. From the amines ea to pea, the interlayer distance increases by about 3.3 Å, i.e. roughly 1 Å per C atom. The somewhat smaller value for $(ipaH)_2Sb_4S_7$ **(3)** compared to $(paH)_2Sb_4S_7$ **(2)** is the result of the nature of the orientation of the amine molecules in the interlayer space (Fig. 5), leading to lower unit-cell volume and higher density for **(3)** compared to **(2)** (Table 1).

The arrangement of the organic cations is reminiscent of the arrangement of amines in intercalated layered clays. In vermiculites with a high layer charge, for example, the alkyl-ammonium ions adopt a paraffin-like orientation, very similar to the arrangement of the protonated amines in compounds **(2)–(5)**, which may therefore be viewed as crystalline host-guest compounds. The orientation of the two crystallographically distinct NH_3 groups with respect to the thioantimonate anions ensures the H atoms are involved in S···H bonding interactions. In compounds **(2)**, **(4)**, and **(5)**, all H atoms have short contacts to the S atoms, whereas in compound **(3)**, one H atom bound to N(1) has no such short contact (Table 4).

A short comparison with the hitherto known compounds containing $[Sb_4S_7]^{2-}$ anions is given here. In the compounds $K_2Sb_4S_7$ [1], $Cs_2Sb_4S_7$ [5], $[Ni(dien)_2]Sb_4S_7 \cdot H_2O$ [39], $(ea)_2[Sb_4S_7]$ [37], and $[Mn(dien)_2]Sb_4S_7$ [40], all S atoms bridge in an $S^{[2]}$ mode as observed in the compounds **(2)–(5)**. In

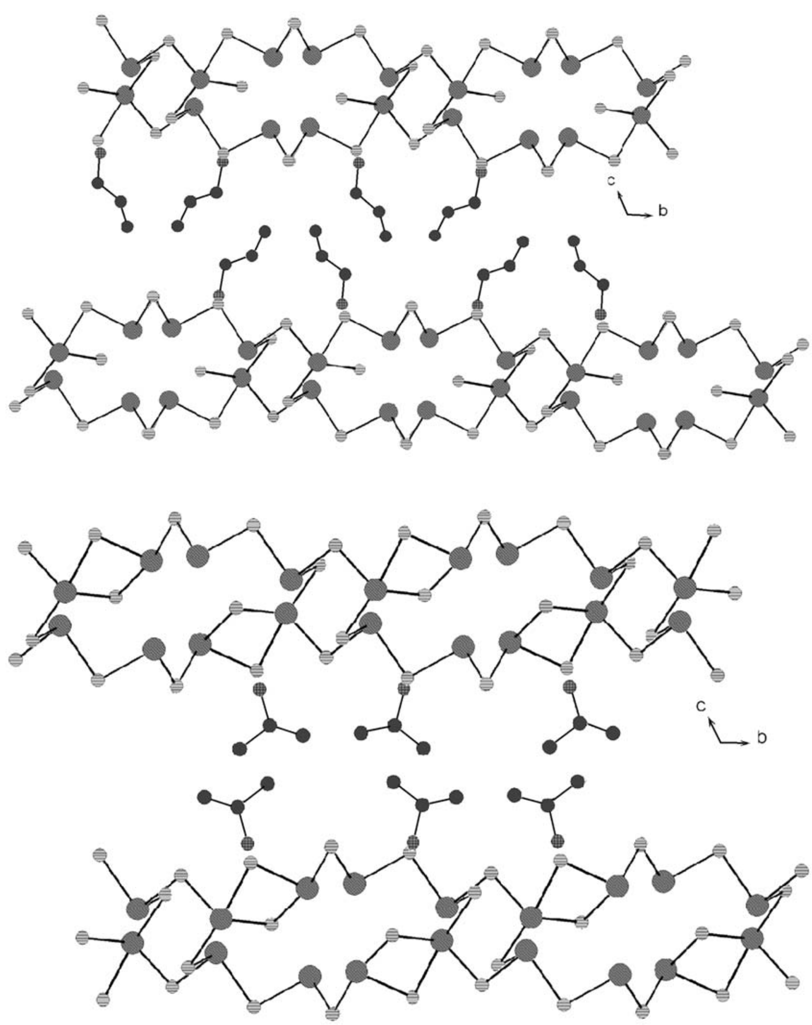

Fig. 5. Stacking of the thioantimonate(III) layers and of the protonated amines in **(2)–(5)**. *n*-propylammonium cations **(2)** (top) and the isopropylammonium cations **(3)** (bottom) are shown as representative examples. Hydrogen atoms are omitted for clarity.

Table 4
Geometric parameters for possible S···H bonds (Å,°) in $(dabH_2)Sb_4S_7$ **(1)**, $(paH)_2Sb_4S_7$ **(2)**, $(i paH)_2Sb_4S_7$ **(3)**, $(baH)_2Sb_4S_7$ **(4)**, and $(peaH)_2Sb_4S_7$ **(5)**.

D–H	d(D–H)	d(H..A)	<DHA	d(D..A)	A
$(dabH_2)Sb_4S_7$ **(1)**					
N1–H1	1.000	2.538	141.94	3.383	S6
N1–H2	1.000	2.397	157.35	3.342	S6 $[x+1, y, z]$
N1–H3	1.000	2.345	166.57	3.326	S2
N2–H1′	1.000	2.210	169.04	3.198	S3 $[-x, -y+2, -z]$
N2–H2′	1.000	2.371	155.17	3.305	S3 $[x, y+1, z]$
N2–H3′	1.000	2.438	148.38	3.331	S3 $[-x+1, -y+2, -z]$
$(paH)_2Sb_4S_7$ **(2)**					
N1–H3N1	0.890	2.413	176.75	3.302	S1 $[x, y-1, z]$
N1–H2N1	0.890	2.418	160.94	3.272	S5
N1–H1N1	0.890	2.698	131.05	3.350	S7 $[-x+1, -y+1, -z+1]$
N2–H1N2	0.890	2.659	164.71	3.526	S2
N2–H2N2	0.890	2.616	167.89	3.491	S4 $[x+1, y, z]$
N2–H3N2	0.890	2.461	174.20	3.347	S6
$(i paH)_2Sb_4S_7$ **(3)**					
N1–H2N1	0.890	2.757	173.70	3.643	S2 $[x, y-1, z]$
N1–H3N1	0.890	2.810	131.57	3.466	S7 $[-x+1, -y+1, -z+1]$
N2–H2N2	0.890	2.723	168.44	3.599	S2
N2–H3N2	0.890	2.585	174.36	3.472	S4 $[x+1, y, z]$
N2–H1N2	0.890	2.440	178.68	3.330	S6
$(baH)_2Sb_4S_7$ **(4)**					
N1–H3N1	0.900	2.638	169.73	3.292	S1 $[x+1, -y+1, -z]$
N1–H2N1	0.900	2.456	151.76	3.277	S5 $[x, y-1, z]$
N1–H1N1	0.900	2.402	135.91	3.344	S7 $[1-x, 1-y, -z]$
N2–H1N2	0.900	2.945	150.44	3.520	S2 $[x+1, y, z]$
N2–H1N2	0.900	2.631	120.33	3.487	S3 $[x+1, y, z]$
N2–H3N2	0.900	2.466	164.02	3.341	S6
N2–H2N2	0.900	2.631	164.03	3.505	S4 $[1+x, y, z]$
$(peaH)_2Sb_4S_7$ **(5)**					
N1–H1A	0.890	2.686	156.07	3.518	S2
N1–H1B	0.890	2.642	164.58	3.508	S4 $[x+1, y, z]$
N1–H1C	0.890	2.440	168.68	3.317	S6
N2–H2A	0.890	2.653	133.24	3.326	S7 $[-x+1, -y+1, -z+1]$
N2–H2B	0.890	2.415	158.18	3.258	S5
N2–H2C	0.890	2.391	178.45	3.280	S1 $[x, y-1, z]$

$K_2Sb_4S_7 \cdot H_2O$ [6] and $Rb_2Sb_4S_7 \cdot H_2O$ [4], besides the $S^{[2]}$ mode, $S^{[3]}$ atoms are also observed. Interestingly, in $Rb_2Sb_4S_7$ [26], there is one $S^{[4]}$ atom and all others act as $S^{[2]}$. The structures of $[Mn(en)_3]Sb_4S_7$ [41], $[Ni(en)_3]Sb_4S_7$ [29], $(pipH_2)[Sb_4S_7]$ [33], $SrSb_4S_7 \cdot 6H_2O$ [7] and $(NH_4)_2Sb_4S_7$ [2] also contain $S^{[2]}$ and $S^{[1]}$ atoms of the same binding mode as those observed in **(1)**. In these last five compounds, one-dimensional $[Sb_4S_7]^{2-}$ chains are observed. Whilst the topologies of the chains in $[M(en)_3]Sb_4S_7$ (M = Mn, Ni, Co) [41], $[Ni(en)_3]Sb_4S_7$ [29], $(pipH_2)[Sb_4S_7]$ [33] and $(NH_4)_2Sb_4S_7$ [2] are significantly different from the topology found in **(1)**, $SrSb_4S_7 \cdot 6H_2O$ [7], exhibits the same connectivity of SbS_3^{3-} and SbS_4^{5-} units as for **(1)** yielding also Sb_2S_2, Sb_3S_3 and Sb_4S_4 heterorings. In a similar manner to the arrangement found in Compound **(1)**, the chains are stacked on top of each other, but adjacent groups of chains are tilted with respect to each other by ca. 90°. The compound $Cs_2Sb_4S_7$ [5] also contains one-dimensional chains, but according to the binding mode of the S atoms they show a different connection mode of the PBUs. The compounds with a layered $[Sb_4S_7]^{2-}$ anion, $[Ni(dien)_2]Sb_4S_7 \cdot H_2O$ [39], $K_2Sb_4S_7 \cdot H_2O$ [6], $Rb_2Sb_4S_7 \cdot H_2O$ [4] and $Rb_2Sb_4S_7$ [26], all have a different connection mode of the PBUs and also different SBUs compared to compounds **(2)–(5)**. This analysis demonstrates the enormous flexibility of the SbS_x units to form a large variety of dimensionalities and topologies even for compounds with an identical Sb:S ratio.

Compound **(1)** decomposes in three closely spaced steps with an extrapolated onset temperature T_e of 214 °C ($T_p = 255$ and 265 °C; Fig. 6). Although the decomposition is accompanied by two signals in the DTA curve, there is some uncertainty in the precise values of the temperatures, owing to the strong overlap

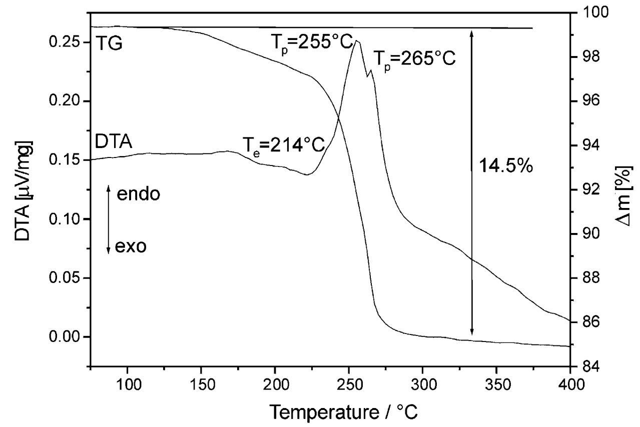

Fig. 6. DTA-TG curves for $(dabH_2)Sb_4S_7$ **(1)** (T_e = extrapolated onset temperature; T_p = peak temperature).

of successive weight-loss steps. The total weight loss amounts to 14.5%. This suggests that, in addition to the loss of the organic component (calculated: 11.0%), decomposition also involves the loss of a mole of sulphur as H_2S (total calculated: 15.2%). We note that the compound **(1)** starts to decompose at ca. 125 °C.

The two compounds, $(paH)_2Sb_4S_7$ **(2)** and $(ipaH)_2Sb_4S_7$ **(3)**, decompose in one step which is accompanied by a strong signal in the DTA curve (Fig. 7). The extrapolated onset temperatures of 230 and 235 °C, respectively are somewhat higher than the value determined for decomposition of **(1)**. The experimental weight loss of 17.8% for **(2)** is in good agreement with the value expected for the emission of the amine and one H_2S molecule (calculated: 17.6%). For Compound **(3)**, there is a slight discrepancy of about 1.9% between the experimentally determined value of 15.7% and that expected for loss of amine plus H_2S (17.6%).

For **(4)**, the decomposition mechanism is more complex and at least two poorly resolved steps can be identified (Fig. 8). The first step starts at $T_e = 208$ °C ($T_p = 223$ °C) and for the second the peak temperature is about 242 °C. Because the two steps overlap, individual mass losses are rather difficult to determine. The total weight change of 19.5% is lower than expected for the removal of the amine and of one H_2S molecule (20.9%).

Finally, the compound of series **(2)–(5)** containing the longest-chain amine, $(peaH)_2Sb_4S_7$ **(5)**, is decomposed in a three-step manner (Fig. 9). The extrapolated onset temperature of the first peak is 171 °C (T_p = 190, 215, 240 °C). Again, the experimental weight loss of 22% is lower than expected for the emission of the organic component and one H_2S molecule (23.4%). The MS spectra recorded during the decomposition of all samples always showed only the signals of the amine fragments and that of H_2S. We note that in the grey residues of the thermal decomposition products, only Sb_2S_3 could be identified with X-ray diffractometry.

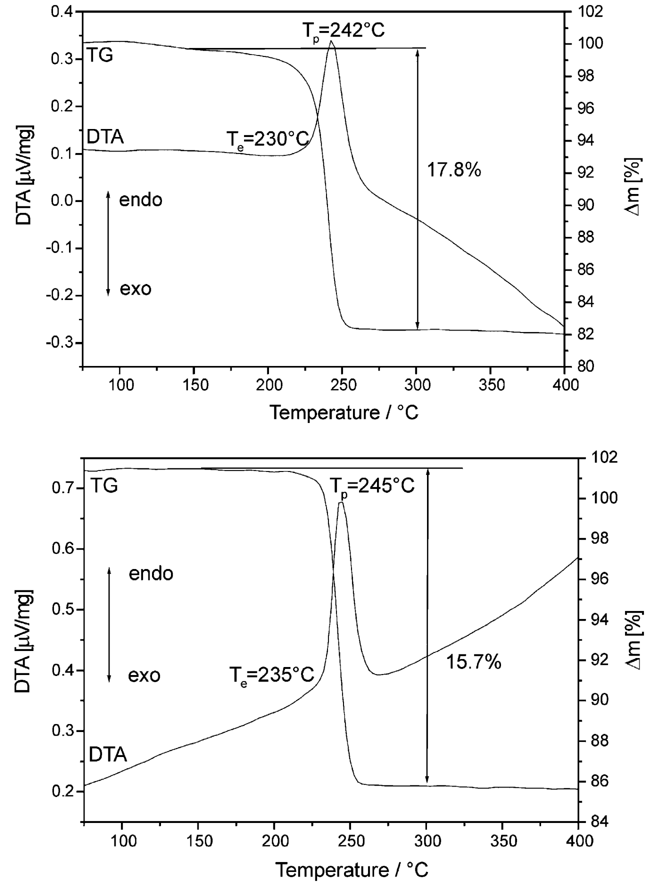

Fig. 7. DTA-TG curves for $(paH)_2Sb_4S_7$ **(2)** (top) and $(ipaH)_2Sb_4S_7$ **(3)** (bottom) (T_e = extrapolated onset temperature; T_p = peak temperature).

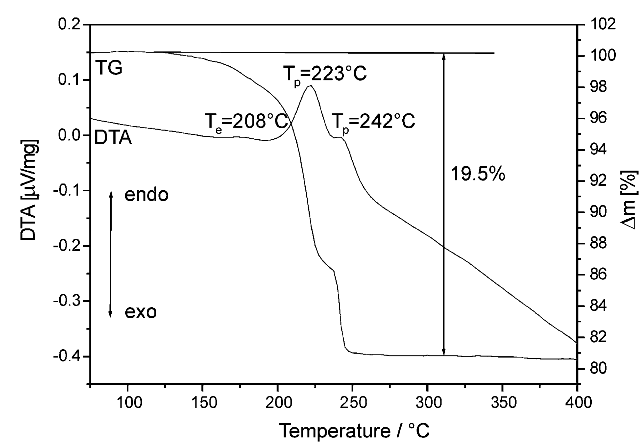

Fig. 8. DTA-TG curves for $(baH)_2Sb_4S_7$ **(4)** (T_e = extrapolated onset temperature; T_p = peak temperature).

The experiments demonstrate that the thermal stability decreases with increasing size of the amine in the compounds. The low T_{onset} of **(1)** relative to **(2)–(5)** is related to the effective lower dimensionality of **(1)**, which consists essentially of isolated double chains with the organic molecules interleaved between them as opposed to

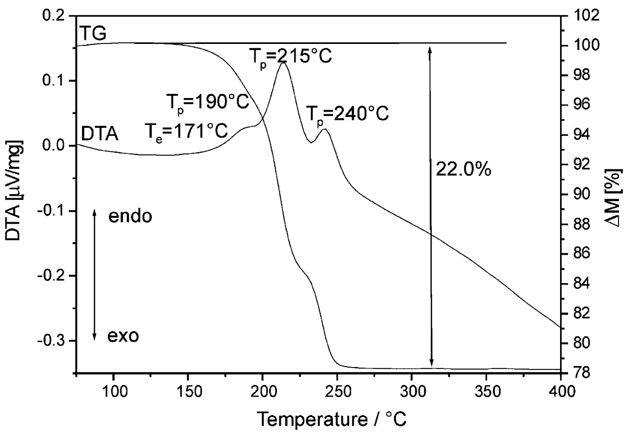

Fig. 9. DTA-TG curves for $(peaH)_2Sb_4S_7$ (**5**) (T_e = extrapolated onset temperature; T_p = peak temperature).

the layer-like structure of **(2)**–**(5)**. The thermal decomposition temperature of **(2)**–**(5)** decreases with increasing number of carbon atoms in the amine and decreasing density. Interactions between the alkyl chains of the amines in the inter-layer galleries are of van der Waals type and with increasing chain lengths the interaction becomes weaker being reflected by the partial disorder of C atoms in compounds **(4)** and **(5)** (see above).

Acknowledgments

AMC thanks The Leverhulme Trust for a Research Fellowship. We also thank the Deutsche Forschungsgemeinschaft (DFG) and the State of Schleswig-Holstein for financial support.

References

[1] H.A. Graf, H. Schäfer, Z. Naturforsch. 27b (1972) 735.
[2] G. Dittmar, H. Schäfer, Z. Anorg. Allg. Chem. 437 (1977) 183.
[3] G. Dittmar, H. Schäfer, Z. Anorg. Allg. Chem. 414 (1975) 211.
[4] G. Dittmar, H. Schäfer, Z. Anorg. Allg. Chem. 441 (1978) 93.
[5] G. Dittmar, H. Schäfer, Z. Anorg. Allg. Chem. 441 (1978) 98.
[6] B. Eisenmann, H. Schäfer, Z. Naturforsch. 34b (1979) 383.
[7] G. Cordier, H. Schäfer, C. Schwidetzky, Z. Naturforsch. 39b (1984) 131.
[8] K. Volk, P. Bickert, R. Kolmer, H. Schäfer, Z. Naturforsch. 34b (1979) 380.
[9] G. Cordier, H. Schäfer, Rev. Chim. Miner. 18 (1981) 218.
[10] G. Cordier, H. Schäfer, C. Schwidetzky, Rev. Chim. Miner. 22 (1985) 722.
[11] M. Schaefer, L. Engelke, W. Bensch, Z. Anorg. Allg. Chem. 629 (2003) 1912.
[12] M. Schaefer, C. Näther, W. Bensch, Solid State Sci. 5 (2003) 1135.
[13] R. Kiebach, W. Bensch, R.-D. Hoffmann, R. Pöttgen, Z. Anorg. Allg. Chem. 629 (2003) 532.
[14] R. Stähler, W. Bensch, Eur. J. Inorg. Chem. 3073 (2001).
[15] W. Bensch, M. Schur, Eur. J. Solid State Inorg. Chem. 33 (1996) 1149.
[16] M. Schur, W. Bensch, Z. Naturforsch. 57b (2002) 1.
[17] W. Bensch, C. Näther, R. Stähler, Chem. Commun. 477 (2001).
[18] R. Stähler, C. Näther, W. Bensch, Eur. J. Inorg. Chem. 1835 (2001).
[19] R. Stähler, W. Bensch, Z. Anorg. Allg. Chem. 628 (2002) 1657.
[20] R. Stähler, C. Näther, W. Bensch, W. Acta Crystallogr. C 57 (2001) 26.
[21] X. Wang, F. Liebau, J. Solid State Chem. 111 (1994) 385.
[22] A.V. Powell, R. Paniagua, P. Vaqueiro, A.M. Chippindale, Chem. Mater. 14 (2002) 1220.
[23] A.V. Powell, S. Boissière, A.M. Chippindale, J. Chem. Soc. Dalton Trans. 4192 (2000).
[24] A. Pfitzner, D. Kurowski, Z. Kristallogr. 215 (2000) 373.
[25] A.V. Powell, S. Boissière, A.M. Chippindale, Chem. Mater. 12 (2000) 182.
[26] W.S. Sheldrick, H.-J. Häusler, Z. Anorg. Allg. Chem. 557 (1988) 195.
[27] R. Stähler, W. Bensch, J. Chem. Soc. Dalton Trans. 2518 (2001).
[28] V. Spetzler, H. Rijnberk, C. Näther, W. Bensch, Z. Anorg. Allg. Chem. 630 (2004) 142.
[29] H.-O. Stephan, M.G. Kanatzidis, Inorg. Chem. 36 (1997) 6050.
[30] M. Schur, C. Näther, W. Bensch Z. Naturforsch. 56b (2001) 79.
[31] X. Wang, A.J. Jacobson, F. Liebau, J. Solid State Chem. 140 (1998) 387.
[32] Y. Ko, K. Tan, J.B. Parise, A. Darovsky, Chem. Mater. 8 (1996) 493.
[33] J.B. Parise, Y. Ko, Chem. Mater. 4 (1992) 1446.
[34] P. Vaqueiro, A.M. Chippindale, A.R. Cowley, A.V. Powell, Inorg. Chem. 42 (2003) 7846.
[35] M. Schur, A. Gruhl, C. Näther, I. Jess, W. Bensch, Z. Naturforsch. 54b (1999) 1524.
[36] L. Engelke, C. Näther, W. Bensch, Eur. J. Inorg. Chem. 2936 (2002).
[37] M. Schur, W. Bensch, Eur. J. Solid State Inorg. Chem. 34 (1997) 457.
[38] R. Stähler, B.-D. Mosel, H. Eckert, W. Bensch, Angew. Chem. 114 (2002) 4671;
R. Stähler, B.-D. Mosel, H. Eckert, W. Bensch, Angew. Chem. Int. Ed. 41 (2002) 4487.
[39] R. Stähler, C. Näther, W. Bensch, J. Solid State Chem. 174 (2003) 264.
[40] M. Schaefer, D. Kurowski, A. Pfitzner, C. Näther, W. Bensch, Acta. Cryst. E 60 (2004) m183.
[41] W. Bensch, M. Schur, Z. Naturforsch. 27b (1996) 405.
[42] G.A. Ozin, Supramolecular Chem 6 (1995) 125.
[43] P. Vaqueiro, D.P. Darlow, A.M. Chippindale, A.V. Powell, Solid State Ionics 172 (2004) 601.
[44] W.S. Sheldrick, J. Chem. Soc. Dalton Trans. 3041 (2000).
[45] G.M. Sheldrick, SHELXS-97, Program for Crystal Structure Determination, University of Göttingen, Germany, 1997.
[46] A. Altomare, G. Cascarano, C. Giacovazzo, A. Guagliardi, M.C. Burla, G. Polidori, M. Camelli, J. Appl. Crystallogr. Sect. A 27 (1994) 435.
[47] G.M. Sheldrick, SHELXL-97, Program for the Refinement of Crystal Structures, University of Göttingen, Germany, 1997.
[48] D.J. Watkin, C.K. Prout, J.R. Carruthers, P.W. Betteridge, R.I. Cooper, Crystals Issue 11; Chemical Crystallography Laboratory, University of Oxford, Oxford, UK, 2001.